

## **Self-cleaning measurements on tiles manufactured with micro-sized photoactive TiO<sub>2</sub>**

\*C.L.Bianchi<sup>1,2</sup>, S. Gatto<sup>1</sup>, S. Nucci<sup>1</sup>, G. Cerrato<sup>2,3</sup> and V. Capucci<sup>4</sup>

<sup>1</sup>) *Università degli Studi di Milano, Dip. Chimica – Milano (Italy)* [claudia.bianchi@unimi.it](mailto:claudia.bianchi@unimi.it)

<sup>2</sup>) *Consorzio INSTM Firenze (Italy)*

<sup>3</sup>) *Università degli Studi di Torino, Dip. Chimica & NIS Centre of Excellence –Torino (Italy)*

<sup>4</sup>) *GranitiFiandre SpA. Castellarano (Italy)*

### **ABSTRACT**

Heterogeneous photocatalysis is a rapidly developing field in environmental engineering. It has a great potential to cope with the increasing pollution in the air. The addition of a photocatalyst to ordinary building materials such as tiles, concrete, paints, creates environmental friendly materials by which air pollution or pollution of the surface itself can be controlled and diminished.

This work reports the results of the laboratory research, especially carried out towards air purifying action and self-cleaning measurements. In particular the research was focused on the study of the photocatalytic behavior of industrially prepared tiles produced starting from commercial micro-sized TiO<sub>2</sub>.

Air purification action has been investigated through NO<sub>x</sub> degradation tests. On the contrary, the degradation of pollution at the surface, also called as self-cleaning action, is verified by the degradation of two different organic dyes: Rhodamine B (red color) and Metanil yellow (yellow).

### **1. INTRODUCTION**

Photocatalysis is based on the double aptitude of the photocatalyst (essentially titania) to simultaneously adsorb both reactants and to absorb efficient photons (Hermann 1999).

The potential benefits of photocatalysis have been reported in a large number of studies published in recent decades. Heterogeneous photocatalysis has been applied in water treatment and air pollution control. A photocatalyst can facilitate the breakdown and removal of a variety of environmental pollutants at room temperature by oxidation, using either sunlight or artificial light as an energy source. In the photo-oxidative removal of potentially toxic organic or inorganic compounds present in the environment, primary attention has been devoted to the role of titanium dioxide (TiO<sub>2</sub>) over compounds such as ZnO, CdS, and WO<sub>3</sub>. This attention is due to its high photocatalytic activity, biological and chemical inertness and stability, resistance to photocorrosion, low cost, nontoxicity, and favorable band-gap energy [Kwon 2008].

Indeed, experimental studies have demonstrated that TiO<sub>2</sub> is the most suitable

photocatalyst of all these compounds for widespread environmental treatment and other applications. These applications include the destruction of microorganisms such as bacteria and viruses, odor control, the conversion of NO<sub>x</sub>, the removal of mercury, the conversion of SO<sub>2</sub>, and the decomposition of oil spills. Furthermore, a TiO<sub>2</sub> photocatalyst that exhibits high activity for the oxidation of volatile organic compounds (VOCs) under ultraviolet (UV) radiation offers an economically and technically practical means to clean air and water (Mehrabi, 2008).

It is well known that VOCs can contribute to the formation of secondary organic aerosols (SOA) particulate matter (PM). As this fraction represents one of the main PM constituents, the ability to break down its precursor would certainly lead to a reduction of PM. Furthermore there is a direct effect as the organic substances present in PM could be oxidized by TiO<sub>2</sub> and transformed into inert compounds. Moreover, both SO<sub>2</sub> and NO<sub>x</sub> are gaseous precursors leading to the formation of secondary PM (ammonium sulfate and ammonium nitrate). As a consequence their degradation could also contribute to PM reduction. In particular, PM degradation could be particularly evident for indoor environment because of the greater permanence of the pollutants due to the limited air exchanges.

The photocatalytic activity of titania is strongly affected by physicochemical features of the particles, with respect to both structural and morphological characteristics. From a structural point of view, TiO<sub>2</sub> can crystallize in three different polymorphic forms: anatase (tetragonal), rutile (tetragonal), and brookite (orthorhombic). The anatase polymorph is generally reported to show the highest photoactivity compared to either brookite or rutile polymorphs because of the low recombination rate of its photogenerated electrons and holes.

However, there appears to be no general agreement on the effect of the particle size on the photocatalytic activity of TiO<sub>2</sub>. Several authors report a peak efficiency, for the given reaction, in correspondence of an optimal particle size. A few examples are mentioned in the following. In the photocatalytic degradation of trichloroethylene in the gas phase with particles (in the 2.3-27 nm range), Maira et al (Maira 2000) found an optimum particle size of 7 nm. Also, in the oxidation of trichloromethene, Zhang et al (Zhang 1998) reported the best efficiency for an anatase size of 11 nm. On the contrary, Almquist and Biswas (Almquist 2002), in the photodegradation of phenol, instead report a much larger optimal particle size in the 25-40 nm range. Furthermore, other authors report a continuous increase in the photocatalytic activity with lowering of the particle size. For example, Anpo et al (Anpo 1987) in the hydrogenation of CH<sub>3</sub>COH report an increase in conversion when the particle size of anatase TiO<sub>2</sub> decreased from 11 to 3.8 nm. The recent results by Lin et al (Lin 2006) are relevant to this debate: the band gap of anatase TiO<sub>2</sub> was observed to decrease monotonically from 3.239 to 3.173 eV when the particle size decreased from 29 to 17 nm and then to increase from 3.173 to 3.289 eV as the particle size decreased from 17 to 3.8 nm, in agreement with the red and blue shifts of the band gap reported by other researchers.

TiO<sub>2</sub> nanoparticles are manufactured worldwide in large quantities to be employed in a wide range of applications, including pigment and cosmetic manufacturing. Although this material is claimed to be chemically inert, TiO<sub>2</sub> nanoparticles can cause negative health effects, such as respiratory tract cancer in rats. Schiestl et al (Schiestl 2009) investigates TiO<sub>2</sub> nanoparticles–induced genotoxicity, oxidative DNA damage,

and inflammation in a mice model.

Even though no specific regulations on nanoparticles exist, but for those covering the same materials in bulk form, responsible companies self-imposed regulations aimed at a correct “handle with care” of the (nano)powders. The main problems are not only connected with the dimensions of the particles: a direct correlation is likely to exist between properties and both shape and surface characteristics of the particles.

Both nano-sized and non-nano-sized TiO<sub>2</sub> exhibit almost the same photochemical performances, but the (pollution) degradation capability of nano-TiO<sub>2</sub> is much greater because of both large specific surface area and high density of surface coordination.

Therefore, the possibility to prepare and use micro-sized TiO<sub>2</sub> opens a new generation of material intrinsically safer than the traditional photocatalytic products for both workers in the factories and public safety.

In the present paper, the industrial preparation of a new generation of photocatalytic tiles is reported. The porcelain gres slabs are prepared with a commercially available photoactive TiO<sub>2</sub> with crystallites larger than the classical nanoparticles usually used in photocatalysis. The final heat treatment at 680°C assures a perfect and stable fixation of the TiO<sub>2</sub> particles.

The photocatalytic properties of this material have been verified through depollution and self-cleaning tests. In details, the pollution degradation of both NO<sub>x</sub> in the gas phase and two different organic dyes directly put at tiles surfaces (Rhodamine B and Metanil yellow) have been investigated.

## **2. EXPERIMENTAL**

### **2.1 Commercial TiO<sub>2</sub> selection**

Two commercially available powdered photoactive TiO<sub>2</sub> were used as standard materials: (i) AEROXIDE® TiO<sub>2</sub> P25 by Evonik Degussa Corporation is the well-known nano-sized TiO<sub>2</sub> characterized by a phase composition of 75:25 anatase:rutile ratio and a surface area of 50 m<sup>2</sup>/g; (ii) 1077 by Kronos was chosen as micro-sized TiO<sub>2</sub>; even if it is not sold as photocatalytic material. This sample consists of pure anatase, specific surface area of ≈ 12 m<sup>2</sup>/g and the absolute lack of ultrafine particles as officially declared by the Company (Kronos 2012) and also checked by us through (HR)TEM measurements (*vide infra*).

### **2.2 Tiles Preparation**

Commercial white tiles produced by GranitiFiandre SpA were covered at the surface with a mixture of micro-sized TiO<sub>2</sub> (Kronos 1077) and a commercial SiO<sub>2</sub>-based compound. In order to ensure the requested product stability, at the end of the preparation procedure tiles were treated at high temperature (min T=680°C) for a convenient time and then brushed to remove the powder present at the surface and that could alter, either artificially increasing or decreasing the photocatalytic performance (sample name: White Ground Active (WGA)).

### 2.3 Samples characterization

Pure powder samples (nano-sized and micro-sized TiO<sub>2</sub> and SiO<sub>2</sub>-based compound) and both photoactive and non-photoactive tiles were fully characterized and the results are reported elsewhere (Bianchi 2012).

In the present paper results from (HR)TEM measurements will be reported to confirm the different sizes of Kronos 1077 in comparison to the standard P25 used as reference. (HR)TEM images were obtained by means of a JEOL 3010-UHR instrument (300 kV acceleration potential; LaB6 filament) equipped with an Oxford INCA X-ray energy dispersive spectrometer (XEDS) with a Pentafet Si(Li) detector. Samples were “dry” dispersed on lacey carbon Cu grids.

### 2.4 Photocatalytic tests

NO<sub>x</sub> degradation was performed in a plant working in static conditions for 6h, using a 10 W/m<sup>2</sup> iron halogenide lamp (Jelosil, model HG 500) emitting in the 315-400 nm wavelength range, photon flux  $2.4 \times 10^{-5} \text{ E dm}^{-3}\text{s}^{-1}$ , checked by actinometry. The degradation was performed at 100, 400 and 1000 ppb, room temperature, RH: 40% (Ardizzone 2007).

Self-cleaning action was followed through the discoloration of dyes directly put at the tiles surfaces, and exposed to the sunlight (Milan – Italy, May 2012). The sunlight power was continuously checked from 9 am to 5 pm every day by a radiometer DeltaOhm HD2102,2, measuring in the range 315 nm to 400 nm from 0.1mW/m<sup>2</sup> to 2000 W/m<sup>2</sup> with a cell diameter of 1 cm. A mean power irradiation value of 7.28 W/m<sup>2</sup> was measured.

Dyes degradation was monitored by Vis-spectrometer equipped with an integrated sphere (OceanOptics, USB4000-VIS-NIR-ES). Calibration: 100% reflectance: BaSO<sub>4</sub> (x=0.3105; y=0.3238; z=0.3658). 0% reflectance: black carbon (x=0,2175; y=0,166; z=0,6035).

Rhodamine B (10g/l) and Metanil yellow (1 g/l) were purchased by Sigma Aldrich and were used without further purification. Samples were dirtied putting at the samples surface 1 µl of the single dye dissolve in water.

The color analysis was performed using the CIEXYZ and CIELAB models as explained afterwards.

## 2. RESULTS AND DISCUSSION

In 1972 Fujishima and Honda (Fujishima 1972) marked the beginning of a new era in heterogeneous catalysis discovering the water splitting on photocatalytic TiO<sub>2</sub> electrodes. Since then, many efforts have been made to understand the fundamental processes and to apply them mainly to environmental cleanup. In fact, it is now well-known the potential application of TiO<sub>2</sub>-based materials for the depollution of air and water.

As discussed in the Introduction, the open question is if only nano-sized TiO<sub>2</sub> particles are active towards the photocatalytic process or if larger-sized particles can also be active. For this purpose, the TiO<sub>2</sub> sample 1077 by Kronos was chosen for this work and the comparison of its morphological features with those of the well-known

P25 is reported in Fig. 1.

The larger size exhibited by the particles of the micro-sized 1077 is evident: in Fig. 1 compare, for instance, the left-hand images in which the general morphology of both P25 and 1077 powders are reported. An accurate inspection of the fringes confirmed the presence of a mixture of anatase/rutile for P25, whereas in the case of the 1077 sample the only polymorph detected is anatase. In particular, the distances among the fringes are ascribable to the spacings ( $d = 0.357$  nm) typical of the (101) anatase crystal planes (see the right-hand image in the bottom section of Fig. 1).

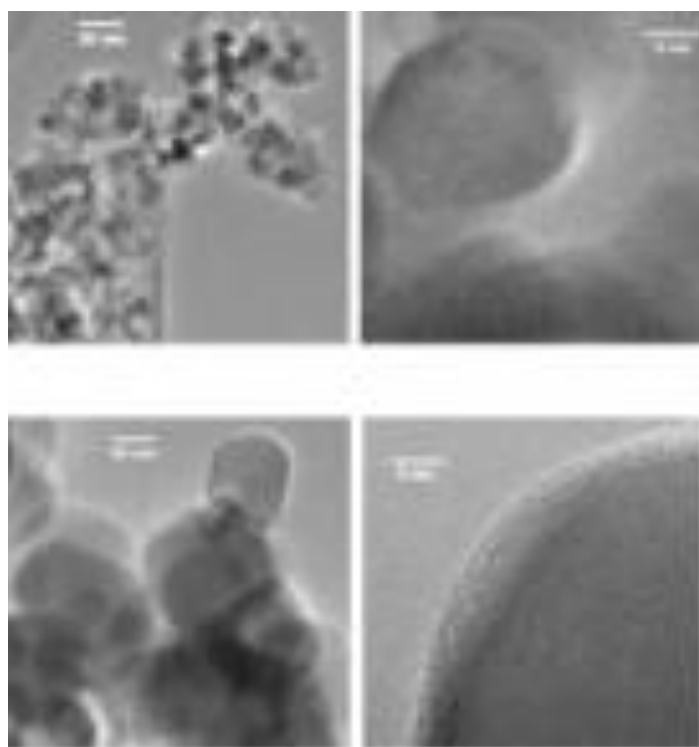


**Fig. 1** TEM images for P25 (top-sections) and 1077 (bottom-sections)

1077 was then used in the industrial production of photocatalytic tiles (see the Experimental section).

One of the most important properties of a photocatalytic material is the possibility to degrade pollutants in the gas phase: in particular, NO<sub>x</sub> is often chosen as reference pollutant to monitor the level of air pollution (WHO 2005).

Figure 2 reports the NO<sub>x</sub> degradation profiles relative to WGA tiles. The NO<sub>x</sub> concentration is the sum of the NO and NO<sub>2</sub> concentrations as the general mechanism for NO<sub>x</sub> degradation by photocatalysis implies the oxidation of the nitric monoxide to nitric or nitrous acid induced by oxygen species produced at the TiO<sub>2</sub> surface

(Ardizzone 2007). The reaction path for NO<sub>x</sub> conversion is generally mediated by OH radicals (Cappelletti 2009):

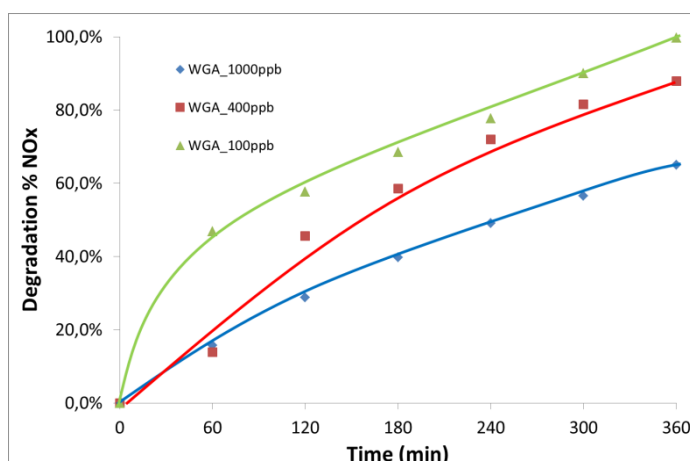


**Fig. 2** NO<sub>x</sub> degradation profiles: tests performed at three different NO<sub>x</sub> concentration in a batch reactor, 10W/m<sup>2</sup>, RH: 40%

It is possible to verify the photocatalytic efficiency of the WGA tiles for all the three pollutant degradation. As expected, the lower is the starting pollution amount, the faster is the NO<sub>x</sub> removal (Bianchi 2012).

The simple depollution properties are often not sufficient to determine the effective potentiality of a photocatalytic material: the achievement of self-cleaning surfaces is then one of the main targets of industrial application of photocatalysis.

To obtain self-cleaning materials with efficient surfaces there are two principal ways: the development of either super-hydrophobic or super-hydrophilic materials. By transferring the microstructure of selected plant surfaces to practical materials like tiles and facade paints, super-hydrophobic surfaces were obtained (Lotus effect). On the contrary, superhydrophilic materials were developed mainly by coating glass, with the semiconducting photocatalyst TiO<sub>2</sub>. If TiO<sub>2</sub> is then illuminated by light, grease, dirt and organic contaminants are decomposed and can easily be swept away by water (rain).

For this purpose, in order to verify once more the WGA photocatalytic properties, these tiles were dirtied with two selected chemical dyes: Rhodamine B, often used as a tracer dye within water, and Metanil yellow, a stuff dye once used also as food color.

Fig. 3 shows the colors disappearance after 5 days of exposure to the sunlight at an UVA mean power of 7.28 W/m<sup>2</sup>.

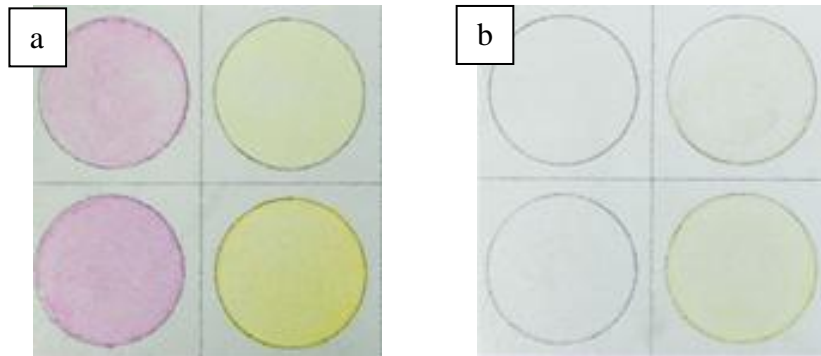


**Fig. 3** WGA tiles dirtied by Rhodamine B and Metanil yellow: a)  $t = 0$ ; b)  $t = 10$  days; solar irradiation (May 2012, UVA mean irradiation power:  $7.28 \text{ W/m}^2$ )

The colors disappearance was also monitored by a spectrophotometer equipped with an integrated sphere following the dye degradation and the return to the starting color of the substrate.

Physiological studies over the years have shown that human eye contains three different types of receptors that respond to short-, mid- and long length light waves. These responses correspond to colors blue, green and red. In the study of color perception, one of the first mathematically defined color spaces is the CIE 1931 XYZ color space, created by the International Commission on Illumination (CIE) in 1931 (CIE 1932), (Smith 1931).

The CIE XYZ color space was derived from a series of experiments done in the late 1920s (Wright 1928; Guild 1931). These experimental results were combined into the specification of the CIE RGB color space, from which the CIE XYZ color space was obtained.

As the human eye possesses three different types of color sensors that are sensitive to different ranges of wavelengths, a full plot of all visible colors is a three-dimensional figure. The CIE XYZ color space was deliberately designed so that the  $Y$  parameter was a measure of the brightness or luminance of a color. The chromaticity of a color was then specified by the two derived parameters  $x$  and  $y$ , two of the three normalized values which are functions of all three tristimulus values  $X$ ,  $Y$ , and  $Z$ :

$$x = \frac{X}{X + Y + Z}$$

$$y = \frac{Y}{X + Y + Z}$$

$$z = \frac{Z}{X + Y + Z} = 1 - x - y$$

The derived color space specified by x, y, and z is known as the **CIE xyY** color space and is widely used to specify colors in practice. An example of CIE xyY graph is reported in Fig.4. The Metanil yellow dye degradation on P25, 1077 and WGA was followed and the relevant results are reported in the blown-up section to Fig. 4.

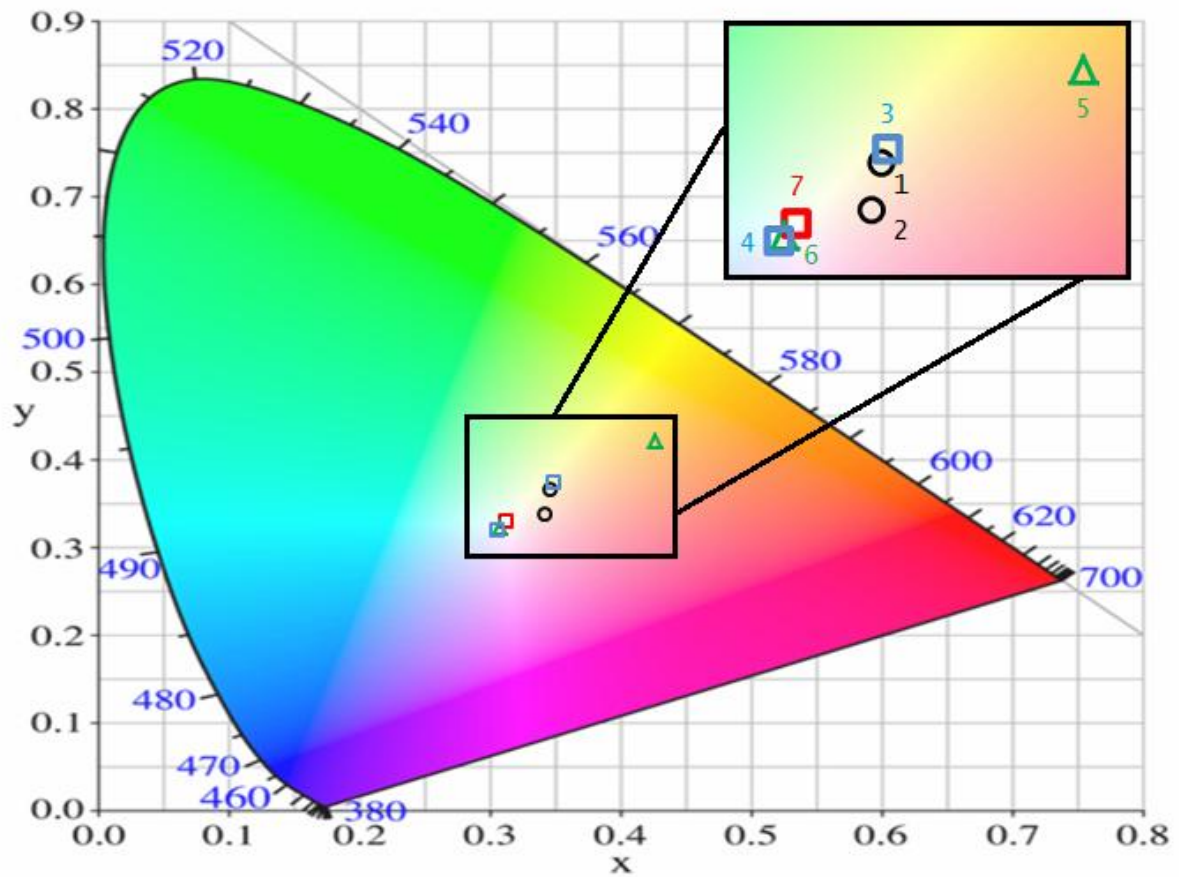


**Fig. 4** CIE xyY graph. The degradation of Metanil yellow is represented in the blown-up section.  $\Delta$  P25;  $\square$  1077;  $\circ$  WGA. The central red square is the Illuminant source D65 (used as reference for absolute white).

It can be observed that the starting color (yellow at  $t = 0$ ) is different among the three samples, underlining that the substrate plays an important role to alter the measure of the color. However, in all cases the color degradation is appreciable.

Detailed values are reported in Table 1 at both starting time (t=0) and at complete disappearance of the color (time depending on both dye and substrate).

Table 1 – XYZ values for Rhodamine B and Metanil yellow at the beginning and at the end of the self-cleaning process under the sunlight.

Dye	Photocatalytic Material	Time (h)	x	y	z
Rhodamine B	WGA	0	0,3248	0,2968	0,3784
	WGA	33	0,3218	0,3344	0,3438
	1077	0	0,3116	0,3261	0,3703
	1077	0.2	0,3098	0,3208	0,3622
	P25	0	0,3215	0,3491	0,3491
	P25	0.1	0,3127	0,3268	0,3606
Metanil Yellow	WGA	0	0,3464	0,3657	0,2879
	WGA	107	0,3427	0,3374	0,3012
	1077	0	0,3489	0,3728	0,2782
	1077	10	0,3061	0,3185	0,3755
	P25	0	0,4268	0,4216	0,1416
	P25	7	0,3074	0,323	0,3696

Rhodamine B is a less resistant dye than Metanil yellow and, notwithstanding it was put on the photocatalytic materials tenfold more concentrated than the yellow dye, its degradation is faster on all the investigated substrates. In particular on the pure TiO<sub>2</sub> powders, both nano and micro-sized, its degradation is complete in few minutes.

Metanil yellow follows a slower degradation process, even if all the substrates exhibit a net self-cleaning action. In particular, WGA shows an efficient self-cleaning action considering that the tiles were irradiated by the sunlight and the UVA mean value was only 7.28 W/m<sup>2</sup> (corresponding to the sun “power” in May 2012 in the Northern Italy).

Data were also elaborated following the CIELAB model (Colorimetry 2004). CIE L\*a\*b\* (CIELAB) is the most complete color space specified by the International Commission on Illumination. It describes all the colors visible to the human eye: it was created to act as an independent model to be used as a reference. The three coordinates of CIELAB represent the lightness of the color (L\* = 0 yields black and L\* = 100 indicates diffuse white; specular white may be higher), its position between red/magenta and green (a\*, negative values indicate green while positive values indicate magenta) and its position between yellow and blue (b\*, negative values indicate blue and positive ones indicate yellow). The CIELAB is, therefore, a color space that has been specifically designed to accurately map color perception. It is commonly used in color manipulation software as it so accurately stores and aids in processing color relationships, like contrast.

Data for WGA dirtied with Rhodamine B are reported in Fig. 5 together with the  $\Delta E^*$  values reported in the inset table. The  $\Delta E^*$  is a single value which takes into account the differences between the  $L^*$ ,  $a^*$  and  $b^*$  of the sample and standard:

$$\Delta E_{ab}^* = \sqrt{(L_2^* - L_1^*)^2 + (a_2^* - a_1^*)^2 + (b_2^* - b_1^*)^2}$$

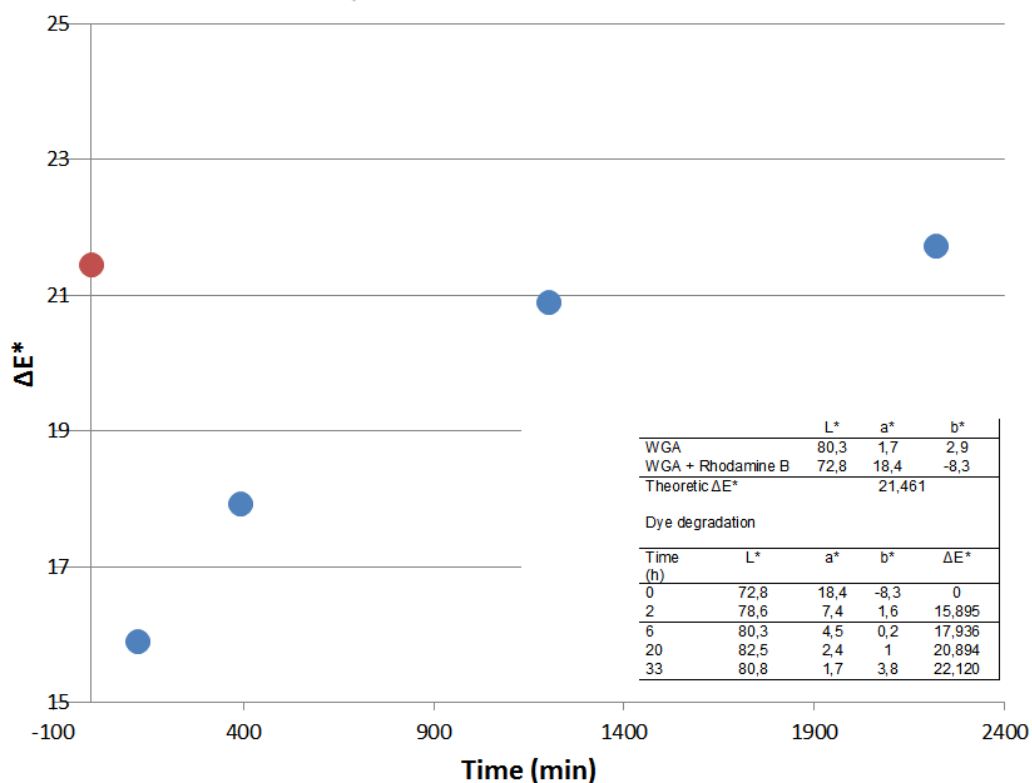


**Fig. 5** - CIELAB elaboration for self-cleaning on WGA with Rhodamine B under the sunlight (UVA mean power  $7.28 \text{ W/m}^2$ ). Blue dots: kinetic of Rhodamine B degradation on WGA. Red dot: WGA starting surface color. In the inset table, all the CIELAB parameters.

## CONCLUSIONS

In the present paper, the photocatalytic performance of two commercial  $\text{TiO}_2$ , respectively nano- and non-nano-sized were checked through depolluting and self-cleaning tests. Both samples exhibit almost the same photochemical performances, even if the pollution degradation capability of nano- $\text{TiO}_2$  is much greater because of both large specific surface area and high density of surface coordination.

This result opens a new generation of material intrinsically safer than the traditional photocatalytic products prepared starting from nano-sized semiconductors. One of this advanced materials, an industrially prepared porcelain gres slab was here tested once more towards both depollution and self-cleaning tests.

The pollution degradation of both  $\text{NO}_x$  in the gas phase and two different organic

dyes directly put at tiles surfaces (Rhodamine B and Metanil yellow) exhibits excellent results confirming the photocatalytic activity of this material.

## REFERENCES

- Almquist C.B., Biswas P. (2002) "Role of Synthesis Method and Particle Size of Nanostructured TiO<sub>2</sub> on Its Photoactivity" *J. Catal.*, **212**, 145-156
- Anpo M., Shima T., Kodama S., Kubokawa Y., (1987) "Photocatalytic hydrogenation of propyne with water on small-particle titania: size quantization effects and reaction intermediates" *J. Phys. Chem.* **91**, 4305-4310
- Ardizzone S., Bianchi C.L., Cappelletti G., Gialanella S., Pirola C., Ragaini V. (2007) "Tailored anatase/brookite nanocrystalline TiO<sub>2</sub>. The optimal particle features for liquid-and-gas-phase photocatalytic reactions" *J. Phys. Chem. C*, **111**, 13222-13231
- Bianchi C.L., Gatto S., Pirola C., Scavini M., Vitali S., Capucci V. (2012) "Micro-TiO<sub>2</sub> As Starting Material For Stable Photocatalytic Tiles", CCC, *submitted*
- Cappelletti G., Ardizzone S., Bianchi C.L., Gialanella S., Naldoni A., Pirola C., Ragaini V. (2009), "Photodegradation of Pollutants in Air: Enhanced Properties of Nano-TiO<sub>2</sub> Prepared by Ultrasound", *Nanoscale Res. Lett.* **4**, 97-105.
- CIE (1932). Commission internationale de l'Eclairage proceedings, 1931. Cambridge University Press, Cambridge
- Colorimetry, 3rd Ed. (2004) CIE 15.3:2004
- Guild J. (1931). "The colorimetric properties of the spectrum". *Philosophical Transactions of the Royal Society of London*, **A230**, 149–187
- Hermann J.-M. (1999), "Heterogeneous photocatalysis: fundamentals and applications to the removal of various types of aqueous pollutants", *Catal Today*, **53**(1), 115–129
- Fujishima A., Honda K., (1972) "Electrochemical Photolysis of Water at a Semiconductor Electrode" *Nature*, **238**, 37-38
- [www.kronos.de](http://www.kronos.de)
- Kwon S., Fan M., Cooper A.T., Yang H. (2008) "Photocatalytic Applications of Micro- and Nano-TiO<sub>2</sub> in Environmental Engineering", *Critical Reviews in Environmental Science and Technology*, **38**, 197-226
- Lin H., Huang C.P., Li W., Ni C., Ismat Shah S., Tseng Y.H., (2006) "Size dependency of nanocrystalline TiO<sub>2</sub> on its optical property and photocatalytic reactivity exemplified by 2-chlorophenol" *Appl. Catal. B*, **68**, 1-11
- Maira A.J., Yeung K.L., Lee C.Y., Yeu P.L., Chan C.K. (2000) "Size Effects in Gas-Phase Photo-oxidation of Trichloroethylene Using Nanometer-Sized TiO<sub>2</sub> Catalysts", *J. Catal.* **192**, 185-196
- Mehrabi S., Barrett C., Thomas C., Watson J., Gray B., Mintz E.A. (2008) "Effect of pH, inorganic ions and wave length on photocatalytic antiviral and antibacterial activities of TiO<sub>2</sub> toward elucidation of the chemistry of the action" From Preprints of Extended Abstracts presented at the ACS National Meeting, American Chemical Society, Division of Environmental Chemistry **48**(1), 864-868

- Smith T., Guild J. (1931) "The C.I.E. colorimetric standards and their use". *Transactions of the Optical Society* **33**(3) 73–134
- Trouiller B., Reliene R., Westbrook A., Solaimani P., Schiestl R.H., (2009) "Titanium dioxide nanoparticles induce DNA damage and genetic instability in vivo in mice", *Cancer Res.*, **69**, 8784-8789  
[http://www.who.int/phe/health\\_topics/outdoorair\\_agg/en/](http://www.who.int/phe/health_topics/outdoorair_agg/en/)
- Wright W.D. (1928). "A re-determination of the trichromatic coefficients of the spectral colours" *Transactions of the Optical Society* **30**(4), 141–164
- Zhang Z., Wang C.C., Zakaria R., Ying J.Y. (1998) "Role of Particle Size in Nanocrystalline TiO<sub>2</sub>-Based Photocatalysts", *J. Phys. Chem. B*, **102**, 10871-10878